Macromolecular Research, Vol. 21, No. 6, pp 636-640 (2013)
DOI 10.1007/s13233-013-1066-x

www.springer.com/13233
pISSN 1598-5032 eISSN 2092-7673

Fabrication of Stable Electrospun TiO_2 Nanorods for High-Performance Dye-Sensitized Solar Cells

Yeong Don Park[†,1], Keita Anabuki[†,2], Sumin Kim[3], Kyung-Won Park[4], Dong Hyun Lee[5], Soong Ho Um[6], Jooyong Kim[*,2], and Jeong Ho Cho[*,6]

[1]*Department of Energy and Chemical Engineering, University of Incheon, Incheon 406-772, Korea*
[2]*Department of Organic Materials and Fiber Engineering, Soongsil University, Seoul 156-743, Korea*
[3]*School of Architecture, Soongsil University, Seoul 156-743, Korea*
[4]*Department of Chemical Engineering, Soongsil University, Seoul 156-743, Korea*
[5]*Department of Polymer Science and Engineering, Dankook University, Gyeonggi 448-701, Korea*
[6]*SKKU Advanced Institute of Nanotechnology (SAINT) and Center for Human Interface Nano Technology (HINT), School of Chemical Engineering, Sungkyunkwan University, Gyeonggi 440-746, Korea*

Received March 22, 2012; Revised July 16, 2012; Accepted July 17, 2012

Abstract: TiO_2 multi-electrodes composed of nanoparticles and nanorods were prepared for use as electrodes in dye-sensitized solar cells (DSSC) in an effort to improve the light-to-electricity conversion efficiency. TiO_2 nanorods have been successfully prepared *via* electrospinning methods using a solution containing titanium isopropoxide (TIP). Acetic acid is generally used as a catalyst in sol-gel processes involving TIP; however, acetic acid induces rapid solidification of the sol solution, resulting in clogging of the nozzle during electrospinning, thereby hindering the mass production of TiO_2 nanorods. In this work, we introduced acetyl acetone as a new catalyst and optimized the electrospinning conditions of TiO_2 nanofibers. The use of acetyl acetone catalysts dramatically extended the solidification time of the TIP sol solution. The DSSC efficiency was improved through the use of TiO_2 multi-electrodes.

Keywords: TiO_2 nanorod, electrospinning, dye-sensitized solar cells (DSSC), sol-gel process, acetyl acetone.

Introduction

Titanium oxide and titanate nanomaterial catalysts are resistant to chemical or photochemical corrosion, are non-toxic, and are low-cost. These materials have been widely used in a variety of applications, including photocatalysts,[1] thin-film solar cells,[2,3] dye-sensitized solar cells (DSSC),[4-11] cosmetics,[12] biomedicine,[13] and ceramics.[14] TiO_2 nanoparticles with large specific surface areas are useful in DSSC applications because they promote the adhesion of dyes. On the other hand, one-dimensional (1D) TiO_2 nanomaterials can potentially improve electron transfer due to their small grain interfaces and light scattering properties, which can enhance the light-to-electricity conversion efficiency.[15-18] In a recent effort to further improve the DSSC efficiency, TiO_2 nanoparticle/nanorod composite electrodes have been designed to offer electron transfer paths without loss of the high surface area for dye adsorption.[19,20]

*Corresponding Authors. E-mails: jhcho94@skku.edu or jykim@ssu.ac.kr
[†]Y. D. Park and K. Anabuki contributed equally to this work.

Several methods for fabricating 1D-structured TiO_2 have recently been reported, including dip-coating, electrospinning, and electrochemical methods.[21-23] Electrospinning is a cost-effective scalable technique with several advantages over other more complicated fabrication methods. It offers a simple approach to producing polymeric inorganic nanofibers with a broad range of diameters, from tens of nanometers to a few micrometers. The fiber structure, morphology, and bead density is easily controlled *via* the processing variables, including the solution concentration, viscosity, surface tension, and conductivity of the solution. Many metal oxide nanofibers and nanotubes, including titanium oxide, silica, cobalt oxide, nickel oxide, tin oxide, zirconium oxide, palladium oxide, and zinc oxide, have been successfully prepared using electrospinning methods.[24,25]

Electrospinnable solutions of metal oxide precursors are prepared by controlling the time-dependent sol-gel reactions of the metal oxide precursors in solution. Acetic acid is generally used as a catalyst; however, this catalyst causes three-dimensional gelation of the precursors, which results in rapid solidification in solution.[26] The instability of the precursor solution then clogs the nozzle during electrospin-

ning, thereby hindering the mass production of metal oxide nanowires *via* electrospinning.

We describe the stable fabrication of TiO_2 nanorods for DSSC electrodes. The fabrication issues were addressed by introducing acetyl acetone as a new catalyst,[27] and the TiO_2 nanofiber electrospinning conditions were optimized. The use of acetyl acetone dramatically extended the solidification time of the TiO_2 gel solution due to the formation of a stable ligand structure between the titanium isopropoxide and the acetyl acetone. The TiO_2 electrodes for use in DSSCs were fabricated by mixing TiO_2 nanorods and the commercially available TiO_2 nanoparticles. The TiO_2 multi-electrodes improved the DSSC efficiency.

Experimental

Preparation of TiO_2 Nanorod. TiO_2 nanorods were prepared by electrospinning, sintering, and mechanical grinding. The electrospinning solution was prepared from titanium isopropoxide (TIP, 3 g), poly(vinyl pyrrolidone) (PVP, 1 g), ethanol (10 mL), and catalysts (acetic acid or acetylacetone, 2 g), followed by stirring at room temperature over a fixed period of time. The viscous solutions were electrospun into fibrous webs under a high voltage of 20 kV with a collective distance of 10 cm between the tip of the needle (diameter 0.61 mm) and the collector. Nanofibers were spun over the course of 2 h. To obtain pure TiO_2 nanofibers, the electrospun nanofibers were sintered at 600 °C for 3 h. The nanofibers were then mechanically ground to form nanorods.

Fabrication of DSSCs. The TiO_2 electrodes for DSSCs were fabricated by mixing the TiO_2 nanorods and commercially available TiO_2 nanoparticles (P-25) in various mixing ratios (0%, 10%, 20%, 30%, 40%, 50%, 75%, and 100%). The mixture of TiO_2 nanorods/nanoparticles (0.2 g), nitric acid (0.4 mL), polyethylene glycol (M_w=6,000, 0.08 g), and one drop of a nonionic surfactant, Triton X-100, was pasted on a fluorine-doped SnO_2 conducting glass (FTO) using the doctor blade method, followed by sintering at 450 °C for 2 h in air (thickness 7 μm). The TiO_2 electrodes were soaked in a 0.5 mM N-719 dye solution in ethanol for 24 h at room temperature. The dye-covered TiO_2 electrode and sputtered Pt counter electrode were assembled into a sandwich-type cell and were sealed with a thermal adhesive film 60 μm thick. The inner space was filled with a liquid electrolyte containing 1-butyl-3-methyl-imidazolium iodide (3.3 mL), iodide (0.1 g), guanidinium thiocyanate (3.9 g), and 4-tert-butylpyridine (2.2 mL) dissolved in a mixture of acetonitrile (18.1 mL), and valeronitrile (3.2 mL). The active area of DSSC cell was 0.25 cm^2.

Characterization. The electrode surface morphologies were imaged using scanning electron microscopy (SEM, JEOL-JSM-6360). ^1H NMR spectra were taken on a Bruker AC200 spectrometer. The TIPs weight loss was monitored as a function of temperature using thermogravimetric analysis (TGA, Mettler Toledo Co., SDTA 851), performed under an inert atmosphere with heating at a rate of 10 °C/min up to a maximum of 900 °C. Photocurrent-voltage characteristics were obtained using a 150 W xenon lamp (Sun 2000 Series Solar Simulators model 11000 source units) to simulate an AM 1.5 G solar (1 Sun condition) irradiance with an intensity of 100 mW/cm^2.

Results and Discussion

The TiO_2 nanorod electrodes for DSSCs were fabricated by electrospinning the TIP precursor solutions into nanofibrous webs using an electrospinning system equipped with a power supply. A high DC voltage was applied between the tip of the needle and the grounded aluminum foil to create an electrostatically charged high-speed jet that emanated from a Taylor cone at the orifice. Prior to reaching the collector, the solvent evaporated from the jet and the solutes solidified and were collected as an interconnected nanofibrous web, as shown in Figure 1.

The surface morphologies of the electrospun TiO_2 nanofibers were investigated by SEM. Figure 1(b) and (c) show SEM images of TiO_2 nanofibrous webs prepared with various TIP sol gelation times. The TIP solution prepared with the acetic acid catalyst and a gelation time of 1 h tended to produce homogeneous and uniformly connected nanofibers with an average diameter of 340 nm. Gelation times greater than 1 h, however, yielded opaque TIP sol solutions due to the excessive degree of hydrolysis and condensation in the solution. The resulting electrospun fibers aggregated into irregular shapes with non-fibrous residues. The TIP sol solution

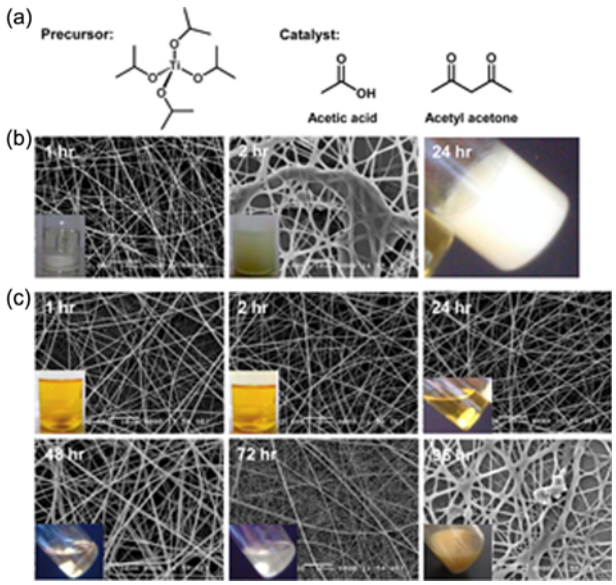

Figure 1. (a) Structures of TIP and the catalysts used for electrospinning the TiO_2 nanofibers. SEM images of the TiO_2 nanofibers prepared using either acetic acid (b) or acetyl acetone (c) as the catalyst.

completely solidified after a gelation time of 24 h, and electrospinning was impossible (Figure 1(b)). The acetyl acetone catalyst dramatically extended the solidification time of the TIP sol solution and enabled the production of homogeneous and stable nanofibers, even after a gelation time of 3 days (Figure 1(c)). As the gelation time increased from 1 to 48 h, the average fiber diameter increased due to the higher viscosity of the sol due to the TIPs polymerization. The electrospun TiO_2 nanofiber morphology was successfully controlled *via* the TIP gelation time. After 72 h, TiO_2 nanofibers with irregular diameters were obtained, and further gelation yielded aggregated fibrous structures. The use of an acetyl acetone catalyst dramatically improved the stability of the TIP sol solution, yielding a long-term electrospinnable TIP sol solution.

The reaction mechanism underlying the polymerization of TIP in the presence of the two catalysts was investigated by ^{1}H NMR. The NMR spectra of the TIP solution containing acetic acid or acetyl acetone are shown in Figure 2. The TIP solutions containing 1:2 molar ratios of TIP to acetic acid or acetyl acetone were examined after 1 h gelation times. The TIP solution containing acetic acid yielded the NMR signal of isopropoxide at δ=4.97-5.04 ppm, much smaller than the signal associated with isopropyl alcohol at 4.08-4.11 ppm and the acetic acid peak at 2.03-2.24 ppm. These results indicated that the four isopropoxide groups of TIP were converted to hydroxyl groups. The three-dimensional multi-gelation of TIP then occurred in solution. The intensity of the isopropoxide peak at 4.73-4.82 ppm, in the TIP solution containing acetyl acetone, was similar to that of isopropyl

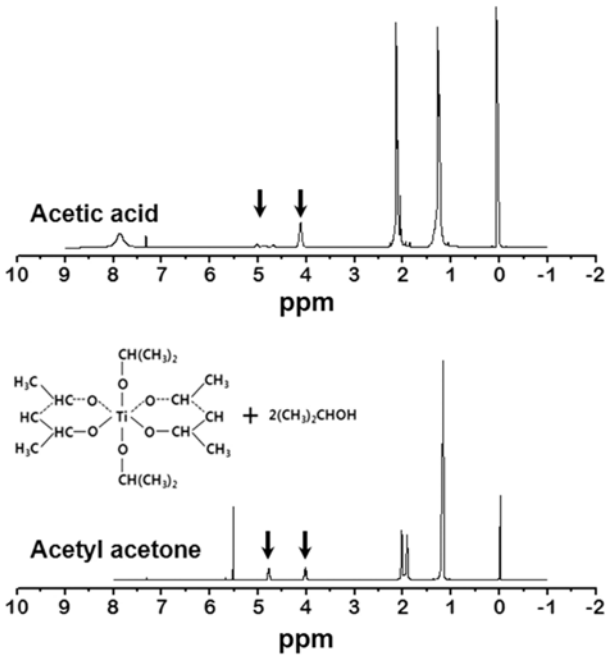

Figure 2. ^{1}H NMR spectra of the TIP solution containing acetic acid or acetyl acetone.

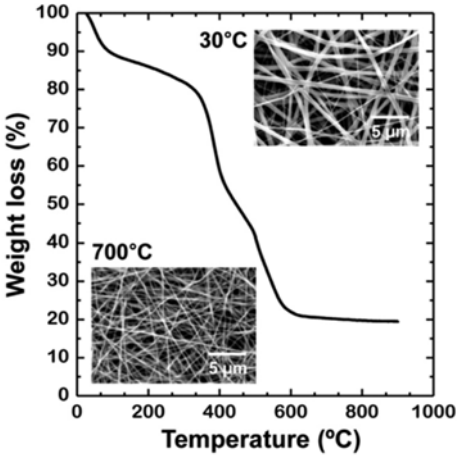

Figure 3. TGA curve for the electrospun TiO_2 nanofibers heated with a heating rate of 10 °C/min. The inset shows SEM images of TiO_2 nanofibers before and after sintering at 700 °C.

alcohol at 3.97-4.06 ppm, indicating the formation of a stable ligand structure between TIP and acetyl acetone, as shown in the inset of Figure 2. This stable ligand produced one-dimensional linear gelation of TIP, which dramatically extended the TIP solidification time in solution.

The thermal behavior of the electrospun TiO_2 nanofibers was examined by TGA (Figure 3). The TGA curve exhibited several weight loss regimes. The first weight loss was observed around 80 °C, corresponding to the evaporation of adsorbed water molecules and isopropyl alcohol formed by the hydrolysis of TIPs. The subsequent weight loss up to a temperature of 350 °C was associated with the volatilization and combustion of organic species, such as PVP and acetyl acetone. Weight loss at temperatures beyond 380 °C corresponded to the crystallization of amorphous residues into mixed anatase and rutile phase.[28,29] The electrospun nanofibers were sintered at 600 °C for 3 h. The average diameter of the sintered nanofibers dramatically decreased, as shown in the inset of Figure 3.[23]

TiO_2 nanorods were obtained by mechanically grinding the sintered nanofibers. The TiO_2 electrodes for use in DSSC were prepared by mixing TiO_2 nanorods with the commercially available TiO_2 nanoparticles. Figure 4 shows SEM images of the TiO_2 multi-electrodes with the different nanorod/nanoparticle ratios. The diameter and length of the grinded nanorods were 320±50 nm and 3.5±1.8 μm, respectively. Although the TiO_2 nanorod content increased, the nanorods were well-dispersed, and no apparent cracks were observed.

The nanorod content in the TiO_2 multi-electrodes used in DSSCs efficiency was tested for its effect on the DSSC efficiency. Figure 5(a) shows the photocurrent-voltage curves of DSSCs containing a variety of nanorod concentrations. The open-circuit voltage (V_{oc}) of a DSSC fabricated based on various TiO_2 electrodes was similar to the TiO_2 nanorod content, indicating that the quasi-Fermi energy state of TiO_2

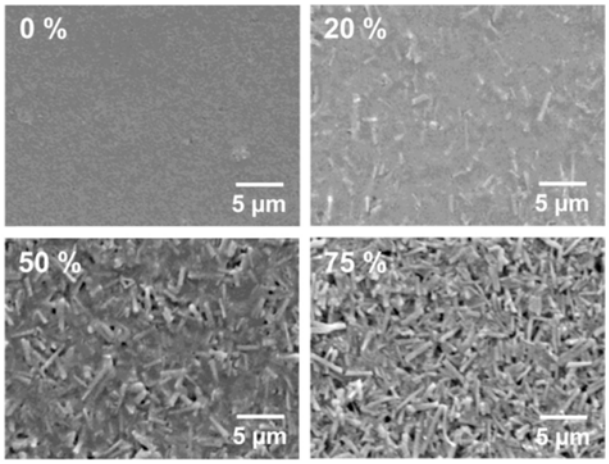

Figure 4. SEM images of the TiO_2 multi-electrodes with different nanorod/nanoparticle ratios (nanorods: 0, 20, 50, and 70 wt%).

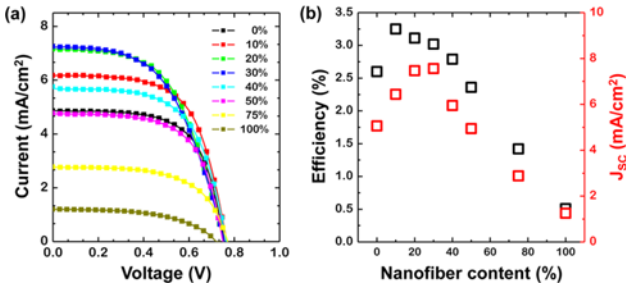

Figure 5. Photocurrent-voltage characteristics of DSSCs fabricated using TiO_2 multi-electrodes with various nanorod/nanoparticle ratios.

was not affected by the presence of the hybrid composite. On the other hand, the short circuit current density (J_{sc}) increased from 5.06 to 7.56 mA/cm^2 until the nanorod content reached a level of 30 wt%. Similarly, the cell efficiency (η) increased from 2.6% to 3.25% with the addition of nanorods up to 10 wt%. These improvements in η and J_{sc} in the DSSCs containing TiO_2 nanorod/nanoparticle multi-electrodes could be explained as follows. The TiO_2 electrode performance in DSSCs depends mainly on both the electron mobility and the specific contact area with the dyes. Electron transport through nanorods is more efficient than through nanoparticle due to their smaller grain interfaces. In contrast, nanoparticles improve the contact with the dyes due to their large specific surface area. At a certain nanorod content, the DSSC performance was maximized. The relationship between the nanowire content and the efficiency is shown in Figure 5(b).

Conclusions

In conclusion, we demonstrated the stable fabrication of TiO_2 nanorods for use as the electrodes in DSSCs. TIP precursor solutions containing an acetyl acetone catalyst were electrospun into nanofibrous webs using an electrospinning technique. The use of acetyl acetone dramatically extended the solidification time of the TIP sol solution due to the formation of a stable ligand structure, producing homogeneous stable nanofibers, even after 3 days. The TiO_2 nanorods were fabricated by electrospinning, sintering, and mechanical grinding of TIP to yield TiO_2 nanorod and nanoparticle electrodes for use in high-performance DSSCs. Care must be taken to control the nanoparticle/nanorod ratios because the TiO_2 electrode performance in DSSC was mainly affected by the electron mobility and the specific contact area with the dyes. A device with a 10 wt% TiO_2 nanorod electrode exhibited a good photovoltaic cell efficiency of 3.25%.

Acknowledgment. This work was supported by the Soongsil University Research Fund of 2010.

References

(1) H. Choi, Y. J. Kim, R. S. Varma, and D. D. Dionysiou, *Chem. Mater.*, **18**, 5377 (2006).
(2) S. H. Park, A. Roy, S. Beaupré, S. Cho, N. Coates, J. S. Moon, D. Moses, M. Leclerc, K. Lee, and A. J. Heeger, *Nat. Photonics*, **3**, 297 (2009).
(3) W. H. Baek, I. Seo, T. S. Yoon, H. H. Lee, C. M. Yun, and Y. S. Kim, *Sol. Energy Mater. Sol. Cells*, **93**, 1587 (2009).
(4) M. Y. Song, D. K. Kim, K. J. Ihn, S. M. Jo, and D. Y. Kim, *Nanotechnology*, **15**, 1861 (2004).
(5) G. K. Mor, K. Shankar, M. Paulose, O. K. Varghese, and C. A. Grimes, *Nano Lett.*, **6**, 215 (2006).
(6) Y. Ohsaki, N. Masaki, T. Kitamura, Y. Wada, T. Okamoto, T. Sekino, K. Niihara, and S. Yanagida, *Phys. Chem. Chem. Phys.*, **7**, 4157 (2005).
(7) M. D. Wei, Y. Konishi, H. S. Zhou, H. Sugihara, and H. Arakawa, *J. Electrochem. Soc.*, **153**, A1232 (2006).
(8) N. Vlachopoulos, P. Liska, J. Augustynski, and M. Gräetzel, *J. Am. Ceram. Soc.*, **110**, 1216 (1988).
(9) B. O'Regan and M. Grätzel, *Nature*, **353**, 737 (1991).
(10) G. K. Mor, K. Shankar, M. Paulose, O. K. Varghese, and C. A. Grimes, *Nano Lett.*, **6**, 215 (2006).
(11) M. Song, J. S. Park, Y. H. Kim, M. A. Karim, S.-H. Jin, R. S. Ree, Y. R. Cho, Y.-S. Gal, and J. W. Lee, *Macromol. Res.*, **19**, 654 (2011).
(12) A. Jaroenworaluck, W. Sunsaneeyametha, N. Kosachan, and R. Stevens, *Surf. Interface Anal.*, **38**, 473 (2006).
(13) J. Schulz, H. Hohenberg, F. Pflücker, E. Gärtner, T. Will, S. Pfeiffer, R. Wepf, V. Wendel, H. Gers-Barlag, and K. P. Wittern, *Adv. Drug Deliv. Rev.*, **54**, 157 (2002).
(14) S. Tursiloadi, H. Imai, and H. Hirashima, *J. Non-Cryst. Solids*, **350**, 271 (2004).
(15) M. Adachi, Y. Murata, J. Takao, J. Jiu, M. Sakamoto, and F. Wang, *J. Am. Chem. Soc.*, **126**, 14943 (2004).
(16) B. Liu and E.S. Aydil, *J. Am. Chem. Soc.*, **131**, 3985 (2009).
(17) S. Uchida, R. Chiba, M. Tomiha, N. Masaki, and M. Shirai, *Electrochemistry*, **70**, 418 (2002).
(18) J.-K. Oh, J.-K. Lee, H.-S. Kim, S.-B. Han, and K.-W. Park,

Chem. Mater., **22**, 1114 (2010).
(19) K. Asagoe, Y. Suzuki, S Ngamsinlapasathian, and S Yoshikawa, *J. Phys. Conf. Ser.,* **61**, 1112 (2007).
(20) V. S. Saji and M. Pyo, *Thin Solid Films*, **518**, 6542 (2010).
(21) M. Y. Song, Y. R. Ahn, S. M. Jo, D. Y. Kim, and J.-P. Ahn, *Appl. Phys. Lett.*, **87**, 113113 (2005).
(22) K. Fujihara, A. Kumar, R. Jose, S. Ramakrishna, and S. Uchida, *Nanotechnology*, **18**, 365709 (2007).
(23) D. Li and Y. Xia, *Nano Lett.*, **3**, 555 (2003).
(24) R. Ramaseshan, S. Sundarrajan, R. Jose, and S. Ramakrishna, *J. Appl. Phys.*, **102**, 111101 (2007).
(25) S.-H. Park, H.-J. Choi, S.-B. Lee, S.-M. Lee, S.-E. Cho, K.-H. Kim, Y.-K. Kim, M.-R. Kim, and J.-K. Lee, *Macromol. Res.*, **19**, 142 (2011).
(26) M. W. Jung, H. J. Oh, J. C. Yang, and Y. G. Shul, *Bull. Korean Chem. Soc.*, **20**, 1394 (1999).
(27) H.-J. Chen, L. Wang, and W.-Y. Chiu, *Mater. Chem. Phys.,* **101**, 12 (2007).
(28) C. Tekmen, A. Suslu, and U. Cocen, *Mater. Lett.,* **62**, 4470 (2008).
(29) R. Parra, M. S. Góes, M. S. Castro, E. Longo, P. R. Bueno, and J. A. Varela, *Chem. Mater.*, **20**, 143 (2008).